

Optical properties of photodetectors based on wurtzite quantum dot arrays

P. Tronc*

Laboratoire d'Optique Physique, Ecole Supérieure de Physique et Chimie Industrielles, 10 rue Vauquelin, 75005 Paris, France

K. S. Zhuravlev and V. G. Mansurov

Institute of Semiconductor Physics, Prospekt Lavrentieva 13, 630090 Novosibirsk, Russia

G. F. Karavaev and S. N. Grinyaev

Kuznetsov Siberian Physicotechnical Institute, Tomsk State University, Pl. Revol'yutsii 1, Tomsk 634050, Russia

I. Milosevic and M. Damnjanovic

Faculty of Physics, University of Beograd, P.O. Box 368, Beograd 11001, Serbia

(Received 7 March 2007; revised manuscript received 6 February 2008; published 21 April 2008)

We show that two types of wurtzite quantum dots can be grown with the C_{3v} symmetry. Their symmetry axis coincides with a threefold proper rotation and a 6_3 improper rotation axis of the wurtzite lattice, respectively. One-, two-, and three-dimensional periodic structures made of such dots are considered. Most of them have the C_{3v} point symmetry except some one- and three-dimensional structures that have the C_{6v} one. The symmetry planes and possible glide planes for the dots and dot structures are those of the wurtzite matrix. It is shown that, under incident light propagating along the growth direction, the absorption is strong for valence-to-conduction-band transitions but, on the contrary, the absorption is weak in infrared detectors based on transitions within the conduction band. It makes it necessary to draw a grating to change the light direction within the device (as is also the case for infrared detectors based on wurtzite quantum wells or superlattices).

DOI: [10.1103/PhysRevB.77.165328](https://doi.org/10.1103/PhysRevB.77.165328)

PACS number(s): 68.65.Hb, 78.67.-n

I. INTRODUCTION

Numerous optoelectronic devices involving quantum dot (QD) arrays are currently under study. For example, in the GaN/AlN system, both intraband and interband transitions are of interest, the former in the infrared wavelength range including fiber-optic telecommunication wavelengths at 1.3 and 1.55 μm ,¹⁻³ the latter in the blue and UV range. In addition, due to the Froelich interaction in highly ionic wurtzite materials, the absorption recovery time is extremely short, of the order of few hundreds of femtoseconds, for intersubband transitions in the GaN/AlGaIn system.^{4,5} Infrared photodetectors based on conduction intersubband transitions in GaN/AlN QD structures have been proposed.^{6,7} Dispersion of QD dimensions naturally arising from growth broadens the detector response range. The devices are generally based on multilayered QD structures. Indeed, QDs cover only a small percentage of the plane surface in a layer and it is useful to increase the number of layers to improve the coupling with the light.⁸ In addition, the structures can be of better quality than those involving a single layer when the few first layers are of lower quality than the following ones.⁹ Last, it is noteworthy that the wurtzite lattice is a polar one. The nanostructures grown along the c axis direction can present a huge built-in electric field arising from the piezoelectric effect and the difference in spontaneous polarizability between the dot and matrix materials.¹⁰

It will be shown hereafter that the wurtzite lattice allows growing two types of high-symmetry dots. Both types have the C_{3v} symmetry. Orientation of the dots is imposed by the matrix lattice that dramatically reduces the number of possible configurations for the QD structures. We consider hereafter the three types of structures, namely, a single chain of

dots stacked one over the other along the c axis of the wurtzite lattice that is chosen as the z axis, a single layer with a regular trigonal or hexagonal distribution of dots within the layer plane, and last, a multilayered structure made of such layers with dots stacked along the c axis and forming chains. Determining the exact symmetry of the dot structures allows deriving the optical selection rules and relative intensities of the transitions. It makes it possible to optimize the design of the photodetectors even if the structures considered hereafter have a rather high symmetry, sometimes higher than that of some grown QD structures. In addition, it will be shown that the possible space-symmetry groups of high-symmetry dot arrays are identical to those of wurtzite quantum wells (QWs) or superlattices (SLs). Therefore, the optical selection rules and hence, in particular, the relative intensities of conduction intersubband transitions are the same.

The present paper is organized as follows. In Sec. II, we analyze the space symmetry of the various QD-based structures as well as the site symmetry of atoms in the lattices and the symmetry lowering by an applied magnetic or electric field. Section III is devoted to establishing the selection rules for dipolar transitions, exciton recombination, infrared absorption, and Raman scattering. Particular attention is paid to infrared photodetectors based on conduction intersubband transitions. It is shown that the transitions between the ground state and the first-excited states are weak with incident light propagating perpendicular to the layers, which makes it necessary to use a grating to change the direction of the light within the device. That is also the case for infrared photodetectors based on conduction intersubband transitions in wurtzite QWs or SLs. The next section deals with the envelope function approximation. Section V considers a few topics such as built-in electric field, distinguishing structures

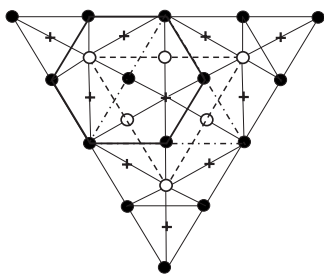


FIG. 1. The wurtzite lattice with a type I dot (thick line) and two type II dots (dashed and dotted-dashed lines, respectively), the latter with the same axis and pointing in the opposite directions. The bases of the two type II dots lie in consecutive monolayers.

with different symmetries, wetting layer effect, and in which ways wurtzite-QD-structure symmetry can be lowered. Section VI provides a brief summary of the results.

II. SYMMETRY ANALYSIS

The wurtzite lattice (C_{6v}^4 nonsymmorphic space group) has a threefold rotation axis and a 6_3 improper rotation (screw) axis. Both axes are parallel to the c direction but do not coincide one with the other. In addition, the 6_3 axis is also a threefold rotation axis. Whereas atoms of the lattice lie on threefold axes, the 6_3 axes do not bear any atom. The three symmetry planes are parallel to the c axis and each of the three glide planes parallel to the c axis is perpendicular to one of the symmetry planes.¹¹ Hereafter, we consider QD structures whose dot and matrix materials are stoichiometric binary compounds with common anion or cation as, for example, GaN/AlN dots. They have the shape of truncated pyramids whose basis lies within the layer plane. From the structure of the wurtzite lattice, it can be predicted that two types of QDs with a threefold symmetry axis can be grown along the c direction: the symmetry axis of type I QDs coincides with a threefold rotation axis of the wurtzite lattice, whereas that of type II QDs coincides with a 6_3 screw axis. The bases of type I dots are hexagons whose sides are perpendicular to the symmetry planes, i.e., parallel to the glide planes parallel to the c axis. The symmetry planes of the dots are those of the wurtzite lattice and the dot symmetry is described by the C_{3v} point group.¹² Hereafter, the labeling of point groups follows Ref. 13. Due to the wurtzite lattice, it is not possible to build hexagonal type II dots (Fig. 1). Nevertheless, it is possible to achieve type II dots with the C_{3v} symmetry (see few examples in Fig. 2). Their three symmetry planes are those of the wurtzite matrix and their shape arises from that of an equilateral triangle. From a layer of the wurtzite lattice, one can grow two subfamilies of identical type II dots that are pointing in opposite directions with respect to the symmetry planes of the wurtzite lattice (Fig. 1). Besides, two identical type II dots grown from two consecutive layers of the wurtzite lattice and having the same symmetry axis are pointing in opposite directions (Fig. 1). Of course, when the size of dots is increased, their shape can be made closer and closer to that of a regular hexagon. In any case, type I and type II dots have the same three symmetry-

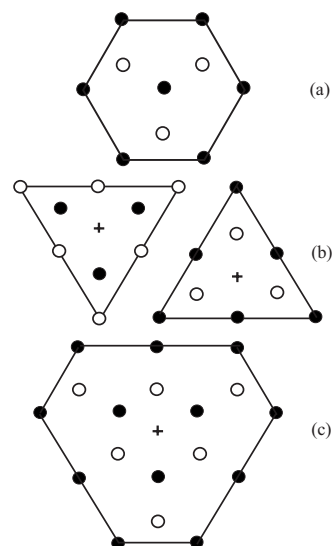


FIG. 2. Examples of (a) type I dot and (b) type II dots, pointing in the opposite directions, and (c) larger type II dot.

plane directions. When analyzing the symmetry of the structures, we adopt the approximation that the atoms are on the sites of a wurtzite lattice with lattice constants being averages between the lattice parameters of dot and matrix materials. Taking this approximation into account, the coordinates of all the atoms in the lattice are well defined and one can determine both the space group and the atomic arrangement over the Wyckoff positions for arbitrary periodic structure.

(1) We consider chains made of dots of the same type only (type I or type II) and having the same symmetry axis. The dots have the same size and shape as well as the same distance between first neighbors. They form a one-dimensional periodic lattice whose space symmetry is described by a rod group or, in more general notations, a line group (hereafter, the labeling of rod and line groups follows Refs. 14 and 15, respectively). Each rod group has the same symmetry operations, except the translations along the x and y axes, as one particular three-dimensional three-periodic space group that will be labeled hereafter as the corresponding group.¹⁶ The one-dimensional Brillouin zone (BZ) of the rod group coincides with the k_z restriction of the BZ of the corresponding three-dimensional three-periodic space group and presents the same symmetry properties as the restriction. Therefore, the irreducible representations (IRs) of the rod groups can be directly taken from the tables of the IRs of the corresponding three-dimensional three-periodic space groups. Within the one-dimensional BZ, the optical selection rules are the same as for the corresponding space group along the k_z axis. The k_z wave vector has to be kept in a direct transition. Let m and n be the numbers of monolayers within a dot and between two adjacent dots, respectively (a monolayer involves a single plane with cations only and a single plane with anions only). For odd values of $m+n$, the 6_3 axis is kept as well as the three glide planes. The unit cell is spread in the z direction over $2(m+n)$ monolayers and involves two dots (pointing in the opposite directions in the case of type II dots). The symmetry of the structure is described by the $R 70$ rod group (or by the line group¹⁷ L_{6H}

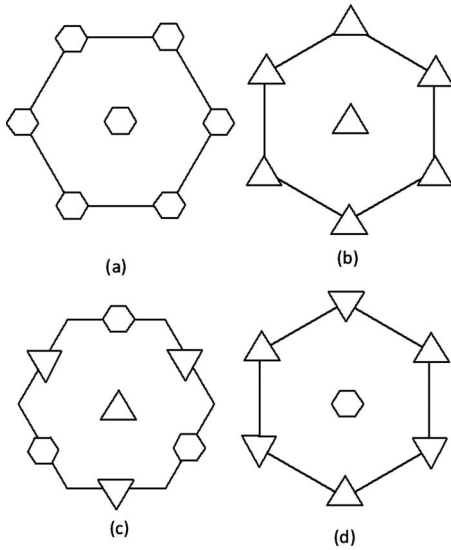


FIG. 3. Single layer with a diperiodic distribution of (a) type I dots and (b) type II dots and (c) and (d) type I and type II dots.

$=T_6^1 C_{3v}$), the corresponding space group being $P6_3mc$ (C_{6v}^4). For even values of $m+n$, the 6_3 axis is replaced by a three-fold rotation axis, the unit cell is spread over $m+n$ monolayers, and the symmetry of the structure is described by the $R 49$ rod group (or by the line group¹⁷ $L_{6H}=T_6^1 C_{3v}$), the corresponding space group being $P3m1$ (C_{3v}^1).

(2) A single layer with a diperiodic distribution of dots within the layer plane can involve both type I and type II dots. Its symmetry is described by a layer group (hereafter, the labeling of layer groups follows Ref. 14). Each layer group has the same symmetry operations, except the translations along the z axis, as one particular three-dimensional three-periodic space group that will be labeled hereafter as the corresponding group.¹⁸ The correspondence between layer groups and three-dimensional three-periodic space groups is provided in Ref. 19. The two-dimensional BZ of the layer group coincides with the (k_x, k_y) restriction of the BZ of the corresponding space group and presents the same symmetry properties as the restriction. In particular, the layer group and its corresponding group have the same point symmetry. The IRs of the little group of the (k_x, k_y) wave vector can be directly taken from the tables of the IRs of the corresponding space group. Within the two-dimensional BZ, the optical selection rules are the same as for the corresponding space group in the (k_x, k_y) plane. The (k_x, k_y) wave vector has to be kept in a direct transition. The 6_3 screw axis of the wurtzite lattice is lifted due to lack of translational symmetry

along the c direction. Among the structures with the highest possible symmetry, one can find structures with a single type of dots and structures with both types of dots. The three symmetry planes of the structure are those of the wurtzite lattice. In layers with a single type of dots only, each dot has six first neighbors [Figs. 3(a) and 3(b)]. In layers where first neighbors are of different types, each type I dot has six type II first neighbors and each type II dot has three first neighbors of each type [Figs. 3(d) and 3(c)]. The symmetry of any of these structures is described by the $L 69$ layer group. The corresponding space group is $P3m1$ (C_{3v}^1).

(3) A multilayered structure is obtained by combining a single layer with chains along the c direction. It is a three-dimensional structure whose symmetry is described by a space group. Depending whether $m+n$ is odd or even, the structures have either the $P6_3mc$ (C_{6v}^4) symmetry, the 6_3 axis and the three glide planes being kept, or the $P3m1$ (C_{3v}^1) symmetry. The unit cell is spread in the z direction over $2(m+n)$ monolayers in the former case and on $m+n$ monolayers in the latter case. Table I displays the space and point symmetries as well as the corresponding group for the various structures.

(4) The site symmetry of an atom in a structure is C_1 (no symmetry) except when the atom is located within a symmetry plane (the site symmetry includes the plane and is described by the C_s (σ_v) point group) or when the atom lies on a threefold symmetry axis of the wurtzite lattice (the site-symmetry group includes the axis and is described by the C_{3v} point group). The latter case occurs only for type I dots.

(5) A uniform magnetic field (axial vector) applied to a structure keeps a symmetry or glide plane (the latter with its improper translation) when perpendicular to it.²⁰ The field keeps also any translation as well as the proper and improper rotations whose axes are parallel to its direction. Besides, the gauge transformations under the symmetry operations deeply modify the symmetry properties of the electron wave functions.²⁰ In QDs and one-periodic structures, such as chains, the symmetry is described by point groups and rod groups, respectively, whatever is the orientation of the field with respect to the structure. In two-periodic structures, the symmetry is described by a rod group when the field lies in the layer plane and by a point group when it does not. In the three-periodic structures, the symmetry is described by a rod group whose axis is parallel to the field.

(6) A uniform electric field keeps a symmetry plane when contained in it. For a glide plane to be kept by the electric field, the latter has to be in the plane and perpendicular to the improper translation, i.e., in the present case, to the c axis. An electric field lifts the translational invariance in the directions that are not perpendicular to it.

TABLE I. Space symmetry and point symmetry (in parentheses) of the various structures.

	Type I or type II dots	Type I and type II dots	Corresponding group
Single chain	Odd $m+n$: $R 70$ (C_{6v}) Even $m+n$: $R 49$ (C_{3v})		C_{6v}^4 C_{3v}^1
Single layer	$L 69$ (C_{3v})	$L 69$ (C_{3v})	C_{3v}^1
Multilayered structure	Odd $m+n$: C_{6v}^4 (C_{6v}) Even $m+n$: C_{3v}^1 (C_{3v})	Odd $m+n$: C_{6v}^4 (C_{6v}) Even $m+n$: C_{3v}^1 (C_{3v})	

III. DIPOLAR OPTICAL SELECTION RULES, EXCITON RADIATIVE RECOMBINATION, INFRARED ABSORPTION, AND RAMAN SCATTERING

Bulk hexagonal GaN and ZnO are direct-gap semiconductors (at the Γ point). The symmetries of the lower conduction band and of the three upper valence bands (the latter in increasing energy ordering) in GaN are described by the Γ_7 , Γ_9 , Γ_7 , and Γ_7 double-valued IRs of the C_{6v}^4 space group, respectively. (Hereafter, the labeling of space group IRs follows Ref. 21. In the labeling, the Γ_5 and Γ_6 IRs are exchanged in comparison with notations common for the II-VI materials.) Note that when the spin-orbit interaction (SOI) is not taken into account, the symmetries of the lower conduction band and of the upper valence bands (there are only two) are described by the Γ_1 , Γ_6 , and Γ_1 single-valued IRs of the C_{6v}^4 space group, respectively.²² With the account of SOI, the Γ_1 IR transforms into Γ_7 , whereas Γ_6 splits into $\Gamma_7+\Gamma_9$. More generally, in wurtzite-based structures, the single-valued IRs transform as follows when taking into account the SOI:

$$\Gamma_{1,2} \rightarrow \Gamma_7, \Gamma_{3,4} \rightarrow \Gamma_8, \Gamma_5 \rightarrow \Gamma_8 + \Gamma_9, \Gamma_6 \rightarrow \Gamma_7 + \Gamma_9$$

(C_{6v}^4 space group),

$$\Gamma_{1,2} \rightarrow \Gamma_6, \Gamma_3 \rightarrow \Gamma_4 + \Gamma_5 \quad (C_{3v}^1 \text{ space group}), \quad (1)$$

where the Γ_4 and Γ_5 IRs of the C_{3v}^1 group are complex conjugate (coreps). They correspond to the same energy level but split under an applied magnetic field.

In ZnO, the symmetries of the lower conduction band and of the three upper valence bands are the same as in GaN, but the ordering in energy of the valence bands is perhaps different. It seems reasonable to assume that the QD-based nanostructures considered in the present work are, like bulk GaN and ZnO, direct-gap semiconductors at the Γ point, except perhaps the structures with very small dots (few monolayer thick) as occurring for some GaAs/AlAs SLs with the zinc blende lattice. It is the reason why our study is focused onto the Γ point for dipolar optical electron transitions. Dipolar optical transitions, exciton radiative recombination, first and second order infrared absorption, and Raman scattering are of interest for both analyzing the electron structure of the dot arrays and defining the way they operate in devices.

A. Dipolar optical transitions

Dipolar optical valence-band-to-conduction-band transitions and exciton radiative recombination have been studied in structures with the C_{6v}^4 space group, such as bulk GaN (Ref. 22) or $(\text{GaN})_m/(\text{AlN})_n$ SLs with odd values of $m+n$,²³ as well as in structures with the C_{3v}^1 space group, such as $(\text{GaN})_m/(\text{AlN})_n$ SLs with even values of $m+n$, or having the C_{3v}^1 group as the corresponding group, such as $(\text{GaN})_m/\text{AlN}$ QWs.²³ The subduction procedure of the Γ IRs of the C_{6v}^4 group onto its C_{3v}^1 subgroup provides the following correspondence:

TABLE II. Kronecker products of the Γ IRs of the C_{3v}^1 group: (a) single-valued IRs and (b) double-valued IRs. The allowed polarizations for electron transitions and exciton radiative recombination are shown in parentheses.

(a)	Γ_1	Γ_2	Γ_3
Γ_1	$\Gamma_1(z)$	Γ_2	$\Gamma_3(x,y)$
Γ_2	Γ_2	$\Gamma_1(z)$	$\Gamma_3(x,y)$
Γ_3	$\Gamma_3(x,y)$	$\Gamma_3(x,y)$	$\Gamma_1(z)+\Gamma_2+\Gamma_3(x,y)$
(b)	Γ_4	Γ_5	Γ_6
Γ_4	Γ_2	$\Gamma_1(z)$	$\Gamma_3(x,y)$
Γ_5	$\Gamma_1(z)$	Γ_2	$\Gamma_3(x,y)$
Γ_6	$\Gamma_3(x,y)$	$\Gamma_3(x,y)$	$\Gamma_1(z)+\Gamma_2+\Gamma_3(x,y)$

$$\Gamma_{1,4} \rightarrow \Gamma_1, \Gamma_{2,3} \rightarrow \Gamma_2, \Gamma_{5,6} \rightarrow \Gamma_3$$

(without the account of the SOI),

$$\Gamma_{7,8} \rightarrow \Gamma_6, \Gamma_9 \rightarrow \Gamma_4 + \Gamma_5 \quad (\text{with the account of the SOI}). \quad (2)$$

The vector representation is $\Gamma_1(z)+\Gamma_6(x,y)$ in the C_{6v}^4 space group and $\Gamma_1(z)+\Gamma_3(x,y)$ in the C_{3v}^1 group. From the Kronecker products of the single-valued IRs and of the double-valued ones, it is possible to get a complete picture of optical transitions together with their relative strength. Indeed, the strong transitions should be allowed even when the SOI is not taken into account, whereas the weak transitions should be allowed only from the SOI. The Kronecker products of single- and double-valued IRs of the C_{6v}^4 group can be found elsewhere²² and those for the C_{3v}^1 group are displayed in Table II. Figure 4 shows the full set of interband transitions both when the SOI is not taken into account and when it is. In the latter case, Fig. 4 provides the relative strength of the various transitions. It is worth noticing that the double-valued IRs describe the only possible wave function symmetries when the SOI is taken into account: there are three in each of both groups. Figure 4 shows that the optical transitions between the two upper valence bands (at least in the case of GaN) and the conduction band are strong in x,y polarization, i.e., with light propagating along the growth direction. It is also the case for the transitions between the valence bands with the exception of the transition between the Γ_7 and Γ_9 states arising from a Γ_6 state in the C_{6v}^4 group.

When designing near-infrared photodetectors, particular attention should be paid to transitions between conduction states since the conduction barrier height allows getting transitions with higher energy than with holes. With the account of the SOI, the ground state in the conduction band has the Γ_7 (Γ_6) symmetry for the systems with the C_{6v}^4 (C_{3v}^1) symmetry. Figure 5 shows the optical selection rules for optical transitions from the conduction ground states in the C_{6v}^4 (C_{3v}^1) group both when the SOI is not taken into account and when it is. In the latter case, Fig. 5 provides the relative strength of the various transitions. With incident light propa-

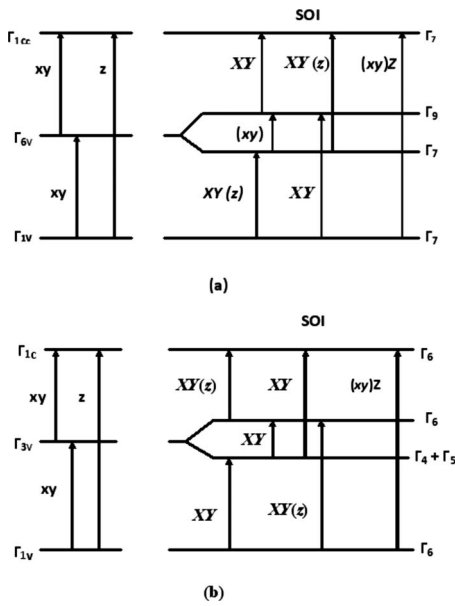


FIG. 4. Symmetry diagrams at the BZ center for the group: (a) C_{6v}^4 and (b) C_{3v}^1 . The polarizations shown in capitals (strong transitions) are allowed both without and with the account of the SOI. The polarizations allowed only from the SOI (weak transitions) are shown in parentheses.

gating along the growth direction, the absorption is strong only for transitions to states arising from a Γ_6 (Γ_3) single-valued symmetry. Computations of band structures for group-III nitrides have appeared in the literature.²⁴ For GaN, for example, when the SOI is not taken into account, the first Γ_6 state in the conduction band is located at 8 eV above the ground Γ_1 state. In between are only two states, with the Γ_3 symmetry, which therefore cannot induce transitions from the ground state (Fig. 5). As a consequence, it likely seems that the first-excited states do not arise from the Γ_6 GaN state. It precludes strong absorption in the x, y polarization between the ground and first-excited states for the structures with the C_{6v}^4 group (generally, in detectors, the first-excited state is located in energy near the top of the barriers). The statement is also valid for structures with the C_{3v}^1 group or corresponding group since only the Γ_3 symmetry arises from the Γ_6 symmetry of the C_{6v}^4 group [Eq. (2)] (Fig. 5). As a consequence, when building a detector structure, it is necessary to draw a grating to change the direction of the light within the device. The above result concerning light polarization for strong absorption has been experimentally demonstrated for GaN/AlN QDs.¹ It is worth noticing that the above conclusions about the optical selection rules and relative intensities of absorption lines also hold for infrared detectors made of QWs or SLs, since the QWs have the C_{3v}^1 group as the corresponding group²³ and the SLs have the C_{3v}^1 or C_{6v}^4 space group depending on the parity of $m+n$.²³ This has been experimentally demonstrated for GaN/AlN.²⁵

B. Infrared absorption and Raman scattering

Selection rules for first and second order infrared absorption and Raman scattering were also studied for structures

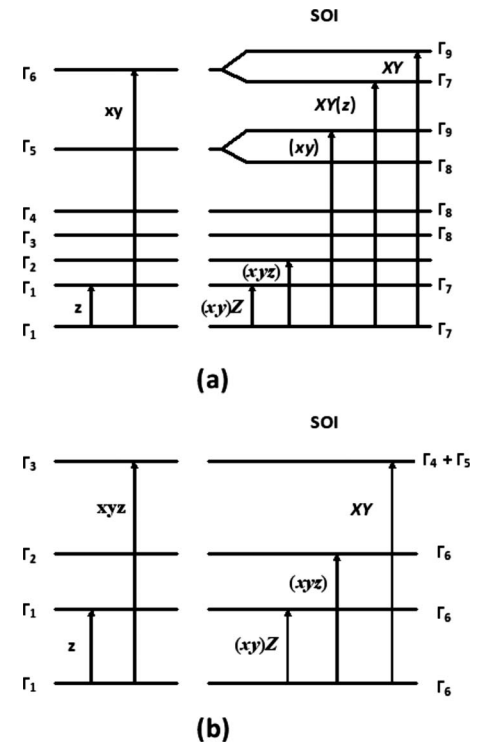


FIG. 5. Symmetry diagrams at the BZ center for the transitions between the conduction ground state and the conduction excited states in the group: (a) C_{6v}^4 and (b) C_{3v}^1 . The polarizations shown in capitals (strong transitions) are allowed both without and with the account of the SOI. The polarizations allowed only from the SOI (weak transitions) are shown in parentheses.

with the symmetries considered in the present work.^{26,27} One can refer to these works to get the selection rules for the dot arrays in the various optical experiments mentioned above. Note, when studying infrared absorption and Raman scattering, that the phonon density of states (DOS) depends on the repartition of the atoms on the Wyckoff positions. The DOS influences the intensities of the lines in the spectra. In structures with the C_{6v}^4 space group or corresponding group, atoms located at any Wyckoff position induce the infrared active phonon modes (the Γ_1 and Γ_6 modes) and the Raman active phonon modes (the Γ_1 , Γ_5 , and Γ_6 modes).²⁸ In structures with the C_{3v}^1 space group or corresponding group, the infrared active phonon modes and the Raman active phonon modes are the same (the Γ_1 and Γ_3 modes) and are induced by atoms located at any Wyckoff position.²⁸

The Froelich interaction characteristics in the considered structures are essentially the same as those in ZnO nanorods and nanotubes.¹¹ Due to the Froelich interaction, the Raman transitions involving the z polarization should be strong. Of course, differences in atomic masses and/or deformation potentials can induce notable changes in the results when going from one material to another.

IV. ENVELOPE FUNCTION APPROXIMATION

When the dimensions of the dots are large compared to the bulk-material unit cell, the dot structures can be studied

by using the envelope function approximation (EFA). EFA models the dots with the help of a potential barrier at the interfaces and the use of effective masses. It is widely accepted that, in wurtzite bulk crystals, the electron effective mass is isotropic, whereas the in-plane and perpendicular hole effective masses are different from each other. In EFA, the symmetry of a type I dot is described by the C_{6v} point group,¹² whereas the symmetry of a type II dot is described by the C_{3v} point group. The symmetry of QD arrays involving type I dots only is described by the C_{6v} point group, whereas the symmetry of arrays involving type II dots only or dots of both types is described by the C_{3v} point group. No space symmetry can be assigned since no crystalline lattice is considered in EFA. Nevertheless, the eigenvalues of the components of the momentum in the direction(s) along which a translational symmetry does exist are good quantum numbers and should be kept in a direct optical transition.

V. DISCUSSION

It should be pointed out that increasing the coupling between dots by lowering their relative distance and/or increasing their size induces formation of energy bands, which lowers the ground electron energy levels but does not change the symmetry of the structure. Besides, several topics should be considered about the dot arrays.

A. Built-in electric field

A huge built-in electric field arising from the piezoelectric effect and the difference in spontaneous polarizability between the dot and matrix materials is expected in the structures.²⁹ The field has been previously studied within single dots.¹² In the structures considered here, the field keeps the translational symmetry and the point symmetry elements (symmetry planes, possible glide planes, and screw axes) in the chains and hence in any structure. As a result, the space symmetry is kept.

B. How to distinguish structures with the C_{6v} and C_{3v} groups

Polarized-light experiments can help in distinguishing dot structures with the C_{6v} point symmetry from those with the C_{3v} symmetry. Indeed, the existence of symmetry and glide planes in the dots (they are those of the wurtzite matrix) can be checked in optical experiments by using a magnetic field perpendicular to the growth direction and rotating the sample around the direction as has been formerly done³⁰ for CdTe/Cd_{1-x}Mn_xTe QWs in photoluminescence experiments. A glide plane is kept under a perpendicular magnetic field and behaves for optical properties as a symmetry plane does, since the improper translation is negligible when compared to optical wavelengths.

C. Wetting layer effect

The effect of a wetting layer has been previously studied within single dots.¹² In valence-to-conduction-band absorp-

tion, most of the electron-hole pairs are created in the layer and flow into the dots since the confinement is generally weaker in the latter along the z direction. At the same time, the recombination energy is reduced.

D. Lowering the array symmetry

One can notice that the orientations of the symmetry and glide planes in the dot arrays are always those of the wurtzite matrix. For small enough values of the n number of monolayers between adjacent dots in a chain, one should expect a strain-induced correlation between the dots³¹ and perhaps a higher chain quality. Threading dislocations are also claimed by various authors to favor layer-to-layer alignment.³² When lowering the symmetry, the glide planes probably disappear first, since they arise not only from the wurtzite lattice but also require odd values of $m+n$. On the contrary, symmetry planes should be at least approximately kept since they are the main features of the lattice (the trigonal or hexagonal shape is close to the roughly circular dot shape exhibited in many transmission electron microscopy diagrams). The statement about symmetry planes holds even if the dots are of various sizes and/or are not stacked one over the other in adjacent QD layers, i.e., do not form periodic chains and/or are displayed at random in the layers. As a consequence, if the distance between adjacent dots is sufficiently large (more than 1 nm) to preclude coupling between them, the dipolar selection rules remain those of the C_{3v} group.

VI. CONCLUSION

We determined the space symmetries of one-, two-, and three-dimensional wurtzite QD arrays. The symmetry planes and possible glide planes of high-symmetry dots and of dot arrays are those of the wurtzite matrix. The 6_3 screw axis of the wurtzite lattice is kept when the sum of the monolayer numbers within a dot and between two consecutive dots, respectively, is odd. The space-symmetry group or the corresponding group of the structure is then C_{6v}^4 . For the other structures, it is C_{3v}^1 . When checked by polarized-light experiments with a magnetic field perpendicular to the c axis, the array symmetry properties can provide a deep insight into the structure of individual dots as well as into their relative configuration. Blue and near UV photodetectors based on dot arrays present natural strong absorption for light propagating along the growth direction, whereas infrared detectors based on transitions within the conduction band require a grating to change the light propagation direction within the device.

ACKNOWLEDGMENTS

We acknowledge grants from the Ministère des Affaires Étrangères (France) (11156RF and 16254YE), the NATO grant (CLG 982207), and the RFBR grants (Russia) (05-02-16901 and 05-02-17259).

*tronc@optique.espci.fr

- ¹Kh. Moumanis, A. Helman, F. Fossard, A. Lusson, and F. H. Julien, *Appl. Phys. Lett.* **82**, 868 (2003).
- ²A. Helman, M. Tchernycheva, Kh. Moumanis, A. Lusson, F. H. Julien, F. Fossard, E. Monroy, B. Daudin, Le Si Dang, B. Damilano, and N. Grandjean, *Phys. Status Solidi C* **1**, 1456 (2004).
- ³Ana Helman, Khalid Moumanis, Maria Tchernycheva, Alain Lusson, Francois Julien, Benjamin Damilano, Nicolas Grandjean, Jean Massies, Christophe Adelman, Frederic Fossard, Daniel Le Si Dang, and Bruno Daudin, in *GaN and Related Alloys*, edited by H. M. Ng, M. Wraback, K. Hiramatsu, and N. Grandjean, MRS Symposia Proceedings No. 798 (Materials Research Society, Pittsburgh, 2004), p. Y5.51.1.
- ⁴N. Iizuka, K. Kaneko, N. Suzuki, T. Asano, S. Noda, and O. Vada, *Appl. Phys. Lett.* **77**, 648 (2000).
- ⁵C. Gmachl, S. V. Frolov, H. M. Ng, S.-N. G. Chu, and A. Y. Cho, *Electron. Lett.* **37**, 378 (2001).
- ⁶L. Doyennette, L. Nevou, M. Tchernycheva, A. Lupu, F. Guillot, E. Monroy, R. Colombelli, and F. H. Julien, *Electron. Lett.* **41**, 1077 (2005).
- ⁷A. Vardi, N. Akopian, G. Bahir, L. Doyennette, M. Tchernycheva, L. Nevou, F. H. Julien, F. Guillot, and E. Monroy, *Appl. Phys. Lett.* **88**, 143101 (2006).
- ⁸B. Damilano, N. Grandjean, F. Semond, J. Massies, and M. Leroux, *Phys. Status Solidi B* **216**, 451 (1999).
- ⁹D. D. Ree, V. G. Mansurov, A. Yu. Nikitin, K. S. Zhuravlev, P. P. Paskov, P.-O. Holtz, and P. Tronc (unpublished).
- ¹⁰T. Bretagnon, P. Lefebvre, P. Valvin, R. Bardoux, T. Guillet, T. Taliercio, B. Gil, N. Grandjean, F. Semond, B. Damilano, A. Dussaigne, and J. Massies, *Phys. Rev. B* **73**, 113304 (2006).
- ¹¹P. Tronc, V. Stevanovic, I. Milosevic, and M. Damnjanovic, *Phys. Status Solidi B* **243**, 1750 (2006).
- ¹²P. Tronc, V. P. Smirnov, and K. S. Zhuravlev, *Phys. Status Solidi B* **241**, 2938 (2004).
- ¹³C. J. Bradley and A. P. Cracknell, *The Mathematical Theory of Symmetry in Solids* (Clarendon, Oxford, 1972).
- ¹⁴*International Tables for Crystallography*, edited by Th. Hahn (Reidel, Dordrecht, 2002), Vol. E.
- ¹⁵I. Milosevic and M. Damnjanovic, *Phys. Rev. B* **47**, 7805 (1993).
- ¹⁶V. P. Smirnov and P. Tronc, *Fiz. Tverd. Tela (S.-Petersburg)* **48**, 1295 (2006).
- ¹⁷I. Milosevic, V. Stevanovic, P. Tronc, and M. Damnjanovic, *J. Phys.: Condens. Matter* **18**, 1939 (2006).
- ¹⁸V. P. Smirnov, R. A. Evarestov, and A. V. Leko, *Fiz. Tverd. Tela (Leningrad)* **27**, 2909 (1985).
- ¹⁹E. A. Woods, *Bell Syst. Tech. J.* **43**, 541 (1964).
- ²⁰P. Tronc and V. P. Smirnov, *Phys. Status Solidi B* **244**, 2010 (2007).
- ²¹S. C. Miller and W. F. Love, *Tables of Irreducible Representations of Space Groups and Corepresentations of Magnetic Space Groups* (Pruett, Boulder, CO, 1967).
- ²²P. Tronc, Yu. E. Kitaev, G. Wang, M. F. Limonov, A. G. Panfilov, and G. Neu, *Phys. Status Solidi B* **216**, 599 (1999).
- ²³Yu. E. Kitaev and P. Tronc, *Phys. Rev. B* **64**, 205312 (2001).
- ²⁴W. R. L. Lambrecht and B. Segall, in *Gallium Nitride*, edited by J. I. Pankove and T. D. Moustakas, *Semiconductors and Semimetals Vol. 50* (Academic, San Diego, 1998), pp. 369–402.
- ²⁵M. Tchernycheva, L. Nevou, L. Doyennette, F. H. Julien, E. Warde, F. Guillot, E. Monroy, E. Bellet-Amalric, T. Remmele, and M. Albrecht, *Phys. Rev. B* **73**, 125347 (2006).
- ²⁶H. Siegle, G. Kaczmarczyk, L. Filippidis, A. P. Litvinchuk, A. Hoffmann, and C. Thomsen, *Phys. Rev. B* **55**, 7000 (1997).
- ²⁷Yu. E. Kitaev, M. F. Limonov, P. Tronc, and G. N. Yushin, *Phys. Rev. B* **57**, 14209 (1998).
- ²⁸M. I. Aroyo, J. M. Perez-Mato, C. Capillas, E. Kroumova, S. Ivantchev, G. Madariaga, A. Kirov, and H. Wondratschek, *Z. Kristallogr.* **221**, 15 (2006).
- ²⁹F. Widmann, J. Simon, N. T. Pelekanos, B. Daudin, G. Feuillet, J. L. Rouviere, and G. Fishman, *Microelectron. J.* **30**, 353 (1999).
- ³⁰Yu. G. Kusrayev, A. V. Koudinov, I. G. Aksyanov, B. P. Zakharchenya, T. Wojtowicz, G. Karczewski, and J. Kossut, *Phys. Rev. Lett.* **82**, 3176 (1999).
- ³¹J. Coraux, H. Renevier, V. Fabre-Nicolin, G. Renaud, and B. Daudin, *Appl. Phys. Lett.* **88**, 153125 (2006).
- ³²J. L. Rouviere, J. Simon, N. Pelekanos, B. Daudin, and G. Feuillet, *Appl. Phys. Lett.* **75**, 2632 (1999).